J|A|C|S
ARTICLES
Published on Web 10/25/2002

Structure-Based Design of Selective Agonists for a Rickets-Associated Mutant of the Vitamin D Receptor

Steve L. Swann,[†] Joel Bergh,[‡] Mary C. Farach-Carson,[‡] Cory A. Ocasio,[†] and John T. Koh*,[†]

Contribution from the Department of Chemistry and Biochemistry, and the Department of Biological Sciences, University of Delaware, Newark, Delaware 19716

Received May 8, 2002

Abstract: The nuclear and steroid hormone receptors function as ligand-dependent transcriptional regulators of diverse sets of genes associated with development and homeostasis. Mutations to the vitamin D receptor (VDR), a member of the nuclear and steroid hormone receptor family, have been linked to human vitamin D-resistant rickets (hVDRR) and result in high serum $1,25(OH)_2D_3$ concentrations and severe bone underdevelopment. Several hVDRR-associated mutants have been localized to the ligand binding domain of VDR and cause a reduction in or loss of ligand binding and ligand-dependent transactivation function. The missense mutation Arg274 → Leu causes a >1000-fold reduction in $1,25(OH)_2D_3$ responsiveness and is, therefore, no longer regulated by physiological concentrations of the hormone. In this study, computer-aided molecular design was used to generate a focused library of nonsteroidal analogues of the VDR agonist LG190155 that were uniquely designed to complement the Arg274 → Leu associated with hVDRR. Half of the designed analogues exhibit substantial activity in the hVDRR-associated mutant, whereas none of the structurally similar control compounds exhibited significant activity. The seven most active designed analogues were more than 16 to 526 times more potent than $1,25(OH)_2D_3$ in the mutant receptor (EC_{50} = 3.3−121 nM). Significantly, the analogues are selective for the nuclear VDR and did not stimulate cellular calcium influx, which is associated with activation of the membrane-associated vitamin D receptor.

The availability of high-resolution protein structures provide us with the unique opportunity to examine the effects of mutations associated with genetic disease at the molecular level. In some rare instances, compounds have been discovered that are able to complement or "rescue" function to genetically impaired proteins.[1−3] Genetic diseases associated with mutations to the nuclear and steroid hormone receptors provide many prototypical examples of mutations that reside adjacent to small molecule binding sites that may be amenable to pharmacological rescue with appropriate hormone analogues. Clearly, not all mutations associated with such diseases can be complemented by small molecules. However, the subset of mutations that directly effect hormone recognition present a unique challenge to chemists to develop compounds that may ultimately provide a novel approach for the development of new treatments for genetic disease.

The superfamily of nuclear/steroid hormone receptors (NHRs) function as ligand-dependent transcriptional regulators of diverse sets of genes associated with development and homeostasis.[4,5] Mutations to various members of the nuclear and steroid hormone receptors are implicated in a broad range of diseases including resistance to thyroid hormone (RTH),[6] leukemia,[7] prostate cancer,[8,9] androgen insensitivity syndrome (AIS),[10] rickets,[11−13] and certain forms of diabetes.[14] In many instances, these mutations reside within or near the binding pocket of the receptor and disrupt normal hormone binding and/or ligand-dependent transactivation function. Screening of existing hormone analogues has yielded compounds that can complement thyroid hormone receptor mutations associated with RTH,[2] androgen receptor mutations found in refractory forms of prostate cancer,[15] and very recently VDR mutations associated

* Corresponding author: E-mail johnkoh@udel.edu.
[†] Department of Chemistry and Biochemistry.
[‡] Department of Biological Sciences.

(1) Foster, B. A.; Coffey, H. A.; Morin, M. J.; Rastinejad, F. *Science* **1999**, *286*, 2507−2510.
(2) Takeda, T.; Suzuki, S.; Lui, R. T.; DeGroot, L. J. *J. Clin. Endocrinol. Metab.* **1995**, *80*, 2033−2040.
(3) Gardezi, S. A.; Nguyen, C.; Malloy, P. J.; Posner, G. H.; Feldman, D.; Peleg, S. *J. Biol. Chem.* **2001**, *276*, 29148−29156.
(4) Aranda, A. A.; Pascual, A. *Phys. Rev.* **2001**, *81*, 1269−1304.
(5) Whitfield, K.; Jurutka, P. W.; Haussler, C. A.; Haussler, M. R. *J. Cell. Biochem.* **1999**, *32*/*33*, 110−122.
(6) Refetoff, S.; Weiss, R. S.; Usala, S. J. *Endocr. Rev.* **1993**, *14*, 348−399.
(7) Gebert, J. F.; Moghal, N.; Frangioni, J. V.; Sugarbaker, D. J.; Beel, B. G. *Oncogene* **1991**, *6*, 1859−1868.
(8) Veldscholte, J.; Ris-Stalpers, C.; Kuiper, G. G. J. M.; Jenster, G.; Berrevoets, C.; Claassen, E.; Vanrooij, H. C. J.; Trapman, J.; Brinkman, A. O.; Mulder, E. *Biochem. Biophys. Res. Commun.* **1990**, *173*, 534−540.
(9) Taplin, M. E.; Bubley, G. L.; Shuster, T. D.; Frantz, M. E.; Spooner, A. E.; Ogata, G. K.; Keer, H. N.; Balk, S. P. *N. Engl. J. Med.* **1995**, *332*, 1393−1398.
(10) Culig, Z.; Hobisch, A.; Hittmair, A.; Cronauer, M. V.; Radmayr, C.; Bartsch, G.; Klocker, H. *Drugs Aging* **1997**, *10*, 50−58.
(11) Hughes, M. R.; Malloy, P. J.; Keiback, D. G.; Kesterson, R. A.; Pike, J. W.; Feldman, D.; O'Malley, B. W. *Science* **1988**, *242*, 1702−1705.
(12) Kristjansson, K.; Rut, A. R.; Hewison, M.; O'Riordan, J. L. H.; Hughes, M. R. *J. Clin. Invest.* **1993**, *92*, 12−16.
(13) Whitfield, G. K.; Selznick, S. H.; Haussler, C. A.; Hsieh, J. C.; Galligan, M. A.; Jurutka, P. W.; Thompson, P. D.; Lee, S. M.; Zerwekh, J. E.; Haussler, M. H. *Mol. Endocrinol.* **1986**, *10*, 1617−1631.
(14) Maslen, G. L.; Williams, T. D.; Lewis, H.; Schafer, A. J.; Chatterjee, V. K.; O'Rahilly, S. *Nature* **1999**, *402*, 880−882.

with rickets.[3] These studies suggest that a subset of NHR-related genetic disorders may be responsive to treatment with appropriate small-molecule analogues. Given the diverse range of mutations associated with certain NHR-related disorders such as AIS, RTH, and rickets, it is unlikely random screens will provide molecular complements to all known mutants. In addition, many hormones act through more than one cellular receptor, as a result of the presence of multiple NHR subtypes or other non-NHR-related receptors. Most hormone analogues reported to activate mutant receptors lack the necessary selectivity to restore activity to the mutationally impaired receptor without adversely interacting with other same-hormone responsive targets. The high-resolution crystal structures of many of the nuclear receptor ligand binding domains may provide a means to rapidly generate selective mutant-complementing analogues by use of structure-based design.

Recent work from our lab has demonstrated that rational molecular design could be used to generate a potent hormone analogue, which selectively activates an RTH-associated mutant of TRβ over the endogenous TRα subtype.[16] Although this initial study focused on a single compound and a single RTH-associated mutant, in principle, this strategy should be applicable to the large number of NHR mutations associated with this general class of genetic disorders. In this study, we explore the generality of our structural-based design approach by synthesizing a focused library of ligands, which were rationally designed to complement a structurally related mutation in the VDR associated with vitamin D-resistant rickets (VDRR).

1.1. Mutations to the VDR Are Responsible for Vitamin D-Resistant Rickets. The hormone 1,25-dihydroxyvitamin D_3 ($1,25(OH)_2D_3$) is responsible for a broad range of physiological effects associated with development and homeostasis. $1,25(OH)_2D_3$ binds and activates the vitamin D receptor (VDR), which functions primarily as a heterodimer with the retinoid X receptor (RXR). Through the VDR, $1,25(OH)_2D_3$ regulates bone remodeling by controlling the expression of osteocalcin and osteopontin, the proliferation and differentiation of osteoblasts,[17] and intestinal calcium and phosphate absorption.[18] In a recent study, the VDR has also been shown to respond to lithocolic acid to regulate expression of cytochrome P450 enzymes, which detoxify hepatotoxic bile acids in the liver and kidneys.[19] Several studies have demonstrated that a second membrane-associated vitamin D receptor is responsible for rapid, membrane-initiated effects of $1,25(OH)_2D_3$ that include monocyte differentiation,[20] bone resorption,[21] PKC and MAP kinase activation,[22] and transcaltachia.[23−26]

Vitamin D-resistant rickets (VDRR) is a genetic disease caused by homozygous autosomal recessive mutations to the vitamin D receptor, which affect DNA binding or normal ligand-dependent transactivation functions of VDR.[11−13] Improper regulation of VDR-responsive genes is associated with high serum concentrations of $1,25(OH)_2D_3$, severe bone underdevelopment, and alopecia. Over 20 mutations to the VDR associated with hVDRR have been reported.[27] Of these mutations, four are found in the ligand-binding domain (LBD) of the receptor. The recently solved cocrystal structure of the ligand binding domain of VDR with $1,25(OH)_2D_3$ has revealed that two of these mutations involve residues that form direct contacts with $1,25(OH)_2D_3$.[28]

One of these mutations, Arg 274 → Leu, causes loss of a critical hydrogen bond to the 1α-OH of $1,25(OH)_2D_3$, which results in a loss of measurable ligand binding in patient fibroblasts and a greater than 1000-fold decrease in in vitro ligand-dependent transactivation function (Figure 1).[12] While transactivation function of VDR(R274L) can be partially restored in vitro by use of extremely high doses of $1,25(OH)_2D_3$, such high concentrations overstimulate other cellular vitamin D- and calcium-dependent biochemical pathways. The other VDRR-associated mutation found within the ligand-binding pocket is His305 → Gln. This mutation is found at the opposite end of the binding pocket, near the C22−C25 side chain of $1,25(OH)_2D_3$, and is associated with a 10−25-fold decrease in $1,25(OH)_2D_3$-dependent transactivation.[29]

Recently, Boehm et al.[30] have reported a series of *non*-steroidal vitamin D mimics that exhibit significant potency and activity in cellular transactivation assays (EC_{50} = 600−40 nM). These mimics, which include LG190155 (EC_{50} = 600 nM), are composed of a bisphenol scaffold and are part of a growing class of nonsteroidal pharmacophores that interact with NHRs (Figure 2). Importantly, these compounds demonstrated reduced membrane VDR-associated cellular calcemic activity compared to that of $1,25(OH)_2D_3$, a characteristic vital for potential therapeutic applications that require selectivity for the nuclear VDR-dependent responses over those associated with the membrane-associated VDR. The simple framework and facile synthesis of these analogues makes them ideal candidates for evaluating our rational design approach to discovering mutation-compensating hormone analogues. Because $1,25(OH)_2D_3$ binds the nuclear VDR in the 6-s-trans conformation and is believed to bind to the membrane-associated receptor in the 6-s-cis conformation, it is reasonable to assume that LG190155 analogues designed to bind to mutant forms of the nuclear receptor will not likely activate the membrane-associated VDR.[26] At this time, however, no detailed structural data have been reported about their precise mode of binding of LG190155 to either receptor.

(15) Taplin, M.-E.; Bubley, G. J.; Ko, Y.-L.; Small, E.; Upton, M.; Rajeshkumar, B.; Balk, S. P. *Cancer Res.* **1999**, *59*, 2511−2515.
(16) Ye, H. F.; O'Reilly, K. E.; Koh, J. T. *J. Am. Chem. Soc.* **2001**, *123*, 1521−1522.
(17) Spiess, Y. H.; Price, P. A.; Deftos, J. L.; Manolagas, S. C. *Endocrinology* **1986**, *118*, 1340−1346.
(18) Chen, T. C.; Castillo, L.; Korycka-Dahl, M.; Deluca, H. F. *J. Nutr.* **1974**, *104*, 1056−1060.
(19) Makishima, M.; Lu, T. T.; Xie, W.; Whitfield, G. K.; Domoto, H.; Evans, R. M.; Haussler, M. R.; Mangelsdorf, D. J. *Nature* **2002**, *296*, 1313−1316.
(20) Bhatia, M.; Kirkland, J. B.; Meckling-Gill, K. A. *Exp. Cell Res.* **1996**, *222*, 61−69.
(21) Farach-Carson, M. C.; Ridall, A. L. *Am. J. Kidney Dis.* **1998**, *31*, 729−742.
(22) Beno, D. W. A.; Brady, L. M.; Bissonnette, M.; Davis, B. H. *J. Biol. Chem.* **1995**, *270*, 3642−3647.
(23) Nemere, I.; Yoshimoto, Y.; Norman, A. W. *Endocrinology* **1984**, *115*, 1476−1483.
(24) Yoshimoto, Y.; Nemere, I.; Norman, A. W. *Endocrinology* **1986**, *118*, 2300−2304.
(25) Zhou, L.-X.; Nemere, I.; Norman, A. W. *J. Bone Miner. Res.* **1992**, *7*, 457−463.
(26) Norman, A. W.; Okamura, W. H.; Hammond, M. W.; Bishop, J. E.; Dormanen, M. C.; Bouillon, R.; van Baelen, H.; Ridall, A. L.; Daane, E.; Khoury, R.; Farach-Carson, M. C. *Mol. Endocrinol.* **1997**, *11*, 1518−1531.
(27) Malloy, P. J.; Pike, J. W.; Feldman, D. *Endocr. Rev.* **1999**, *20*, 156−188.
(28) Rochel, N.; Wurtz, J. M.; Mitschler, A.; Klaholz, B.; Moras, D. *Mol. Cell.* **2000**, *5*, 173−179.
(29) Malloy, P. J.; Eccleshall, T. R.; Gross, C.; Van Maldergem, L.; Bouillon, R.; Feldman, D. *J. Clin. Invest.* **1997**, *99*, 297−304.
(30) Boehm, M. F.; Fitzgerald, P.; Zou, A.; Elgort, M. G.; Bischoff, E. D.; Mere, L.; Mais, D. E.; Bissonnette, R. P.; Heyman, R. A.; Nadzan, A. M.; Reichman, M.; Allegretto, E. A. *Chem. Biol.* **1999**, *6*, 265−275.
(31) Norman, A. W.; Ishizuka, S.; Okamura, W. H. *J. Steroid Biochem. Mol. Biol.* **2001**, *76*, 49−59.

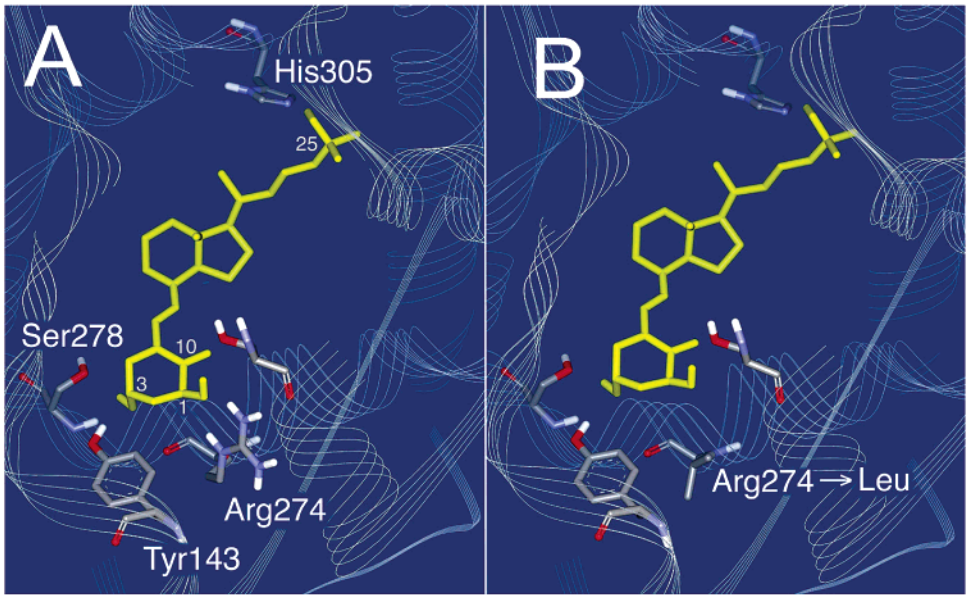

Figure 1. (A) Key polar interactions between $1,25(OH)_2D_3$ and *h*VDR based on the reported cocrystal structure.[28] (B) Modeled structure of $1,25(OH)_2D_3$ in a site model of the VDRR-associated mutant *h*VDR(R274L).

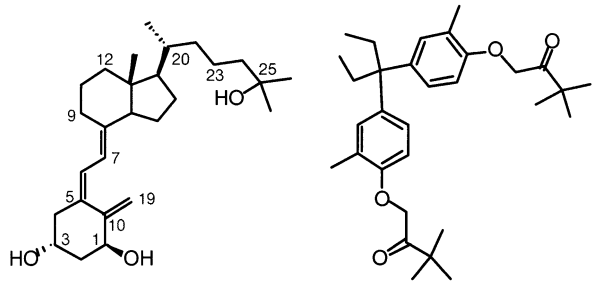

$1,25(OH)_2D_3$ **LG190155**

Figure 2. Structure of $1,25(OH)_2D_3$ and the agonist LG190155.

Results and Discussion

2.1. Docking of LG190155 in VDR(wt) and VDR(R274L). To gain insights into the structural elements responsible for the high-affinity binding of LG190155 in VDR, binding-site models based on the published coordinates of the "wild-type" VDR/$1,25(OH)_2D_3$ cocrystal structure were constructed and studied computationally (Flo/Qxp, Thistlesoft).[28,32] The site model included all residues within 10 Å of the bound $1,25(OH)_2D_3$ and allowed all residues in contact with the ligand to be flexible during simulations. The ligand-dependent transactivation by nuclear hormone receptors represents a complex sequence of molecular events, which includes a substantial structural reorganization of the receptor upon ligand binding, and is often coupled to dimerization, DNA binding and the association of coactivators.[33,34] Therefore, calculations based on constrained site models based on the agonist-bound structure of VDR are not expected to represent the complex series of events involved in ligand-dependent transactivation function. However, a ligand's ability to efficiently bind to models of the agonist-bound receptor may be viewed as a prerequisite for transactivation function and has been used to successfully design agonists selective for mutant forms of NHRs.[16,35]

The validity of our model was supported by the observation that simulated Monte Carlo docking of $1,25(OH)_2D_3$, starting from random conformations and orientations of the ligand, faithfully generated global minima virtually superimposable with the published X-ray coordinates of the ligand-bound complex. A 1000-step Monte Carlo docking search of LG190155 into the VDR(wt) binding site model yielded only one consensus ligand orientation and conformation within 1.3 kcal/mol of the global minimum. The modeled structure showed that LG190155 occupied a similar space within the binding pocket as $1,25(OH)_2D_3$ (Figure 3). The symmetric ligand places one of the 3,3-dimethyl-2-butanone groups in the same space occupied by the C22−C25 side chain of $1,25(OH)_2D_3$, forming a hydrogen bond to His305. The other 3,3-dimethyl-2-butanone group occupies the same space usually occupied by C3−C5 of the A-ring of $1,25(OH)_2D_3$, where the carbonyl oxygen hydrogen-bonds to the side chain of Ser278 and Tyr143, analogous to the 3β-hydroxyl of $1,25(OH)_2D_3$. Interestingly, our model suggests that LG190155 does not directly interact with Arg274, the hydrogen-bonding partner of the 1α-OH of $1,25(OH)_2D_3$. This model is, therefore, consistent with the observation that LG190155 does not show a reduction in activity in the mutant VDR(R274L) (vide infra). The convergence of our docking simulations on a single structure, combined with the consistency of its biological activity in the mutant, strongly supports the validity of our modeled structure.

The structure of the mutant receptor VDR(R274L) has not been reported; therefore, a binding-site model of this mutant was generated by changing the side chain of Arg274 to that of leucine and using a conformation search to place the side chain in its lowest energy conformation within the neighboring residues. There was no evidence that the leucine side chain would prevent the proper folding of the receptor in its agonist-

(32) McMartin, C.; Bohacek, R. J. *Comput.-Aided Mol. Des.* **1997**, *11*, 333−344.
(33) Collingwood, T. N.; Urnov, F. D.; Wolffe, A. P. *J. Mol. Endocrinol.* **1999**, *23*, 255−275.
(34) MacDonald, P. N.; Baudino, T. A.; Tokumaru, H.; Dowd, D. R.; Zhang, C. *Steroids* **2001**, *66*, 171−176.
(35) Shi, Y.; Koh, J. T. *Chem. Biol.* **2001**, *8*, 501−510.

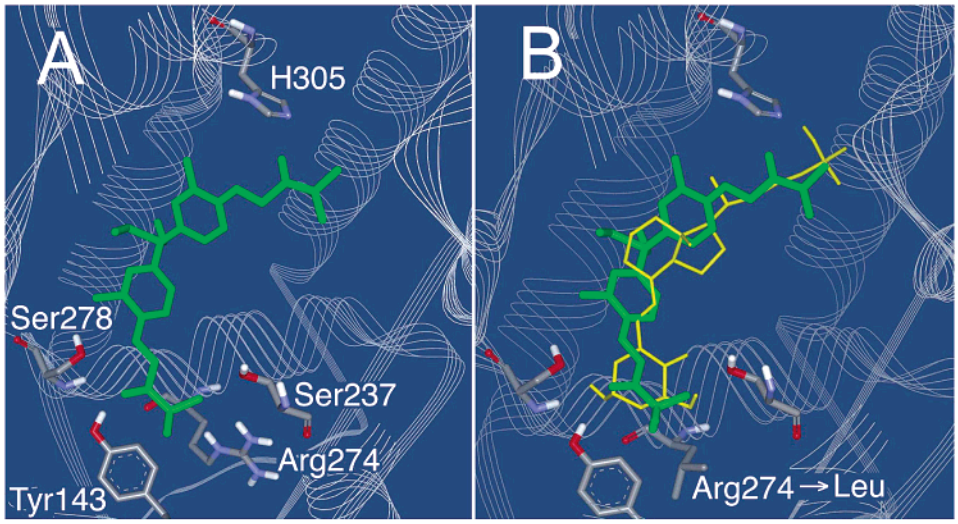

Figure 3. (A) Modeled structure of LG190155 in binding-site model of VDR(wt). (B) Modeled structure of LG190155 (green) and 1,25$(OH)_2D_3$ (yellow) in binding-site model of VDR(R274L).

bound conformation. The Arg274 → Leu mutation opens a large hydrophobic cleft or "hole" within the binding pocket in the space formerly occupied by the guanidine of Arg274. Monte Carlo docking simulations of both 1,25$(OH)_2D_3$ and LG190155 show no significant changes in overall positions and conformations of these ligands when docked in the VDR(R274L) mutant compared to their calculated structures in VDR(wt). Apparent association energies (E_{assn}) calculated for 1,25$(OH)_2D_3$ in both VDR(wt) and VDR(R274L) show a decrease in affinity for the mutant ($\Delta E_{assn} = +1.5$ kcal/mol) consistent with the experimentally observed loss in transcriptional potency [EC_{50}(R274L)/EC_{50}(wt) = 0.1%]. LG190155 does not utilize Arg274 as a hydrogen-bond partner and does not show a decrease in its calculated apparent association energy [E_{assn}(wt) = −9.0 kcal; E_{assn}(R274L) = −9.5 kcal], nor does it show a decrease in transcriptional potency for the mutant [EC_{50}(wt) = 110 nM, EC_{50}(R274L) = 60 nM]. Taken together, these observations strongly support our binding-site model of the VDR(R274L) mutant as a reasonable basis for structure-based ligand design.

2.2. Rationale for Ligands Designed To Complement VDR (R274L). We envisioned that one of the 3,3-dimethyl-2-butanone groups of LG190155 could be replaced with appropriate functionality to complement the unique binding site presented by the VDR(R274L) mutant (Figure 4). Previously, we demonstrated that replacement of a carboxylate of a thyroid hormone analogue with a neutral polar alcohol effectively complemented an Arg320 → Cys mutation of the homologous residue in TRβ associated with resistance to thyroid hormone (RTH).[16] A neutral hydrophobic appendage to the core structure of LG190155 of appropriate size could be used to form new hydrophobic contacts with the modified receptor in a manner analogous to that used to complement the RTH-associated mutation in TRβ(R320C). Chemically similar modifications were also recently used to complement an artificial Arg14 → Ala mutant in kinesin.[36,37] The facile synthesis of LG190155 analogues from compound **1** permitted us to rapidly generate new analogues from commercially available alkylating agents

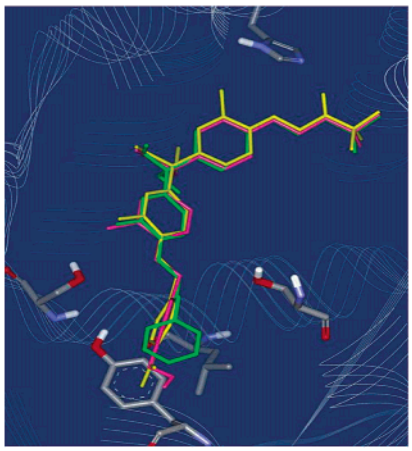

Figure 4. Overlay of modeled LG190155 analogues (A-11, A-9, and A-6) designed to complement VDR(R274L).

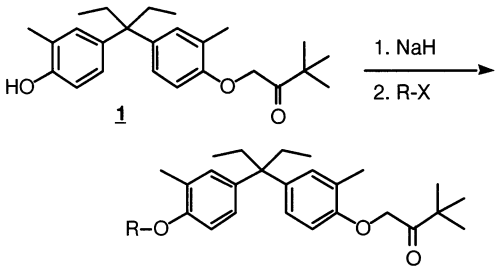

Figure 5. Synthesis of LG190155 analogues from simple alkylating agents.

and simple derivatives thereof (Figure 5). However, far more chemically compatible alkylating agents are commercially available than could be reasonably and affordably synthesized and screened. Therefore, molecular modeling was used to perform a virtual screen of the best candidate compounds. The virtual screening of agonist analogues allowed us to further evaluate the general effectiveness of our structure-based design approach to molecular complementation.

Over 100 commercially available alkyl halides were initially considered for this study. Visual inspection of the binding site model suggested that 40 of the reagents would afford analogues having appropriate molecular volumes and lipophilicity

(36) Kapoor, T. M.; Mitchison, T. J. *Proc. Natl. Acad. Sci. U.S.A.* **1999**, *96*, 9106−9111.
(37) Koh, J. T. *Chem. Biol.* **2002**, *9*, 17−23.

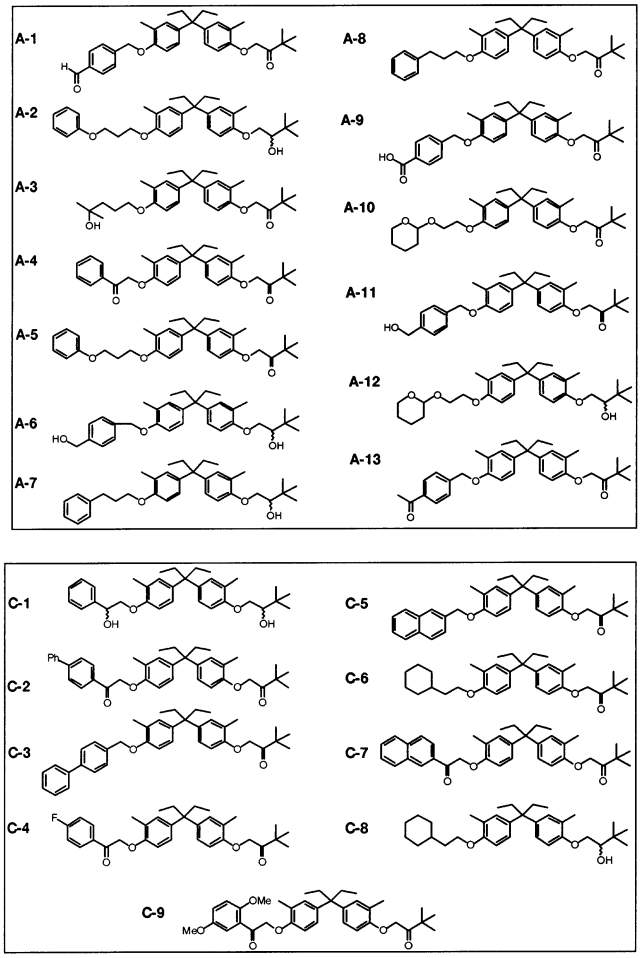

Figure 6. (Top panel) Analogues (A-1 to A-13) predicted by molecular modeling to have high affinity for agonized conformation of VDR(R274L). (Bottom panel) Control compounds (C-1 to C-9) predicted not to have high affinity for the agonized conformation of VDR(R275L).

to be considered as potential mutant-specific agonists for VDR(R274L). Bisphenol analogues containing these 40 candidate appendages were subjected to comprehensive Monte Carlo docking simulations, which explored both random conformations and orientation of each compound in our VDR(R274L) binding site model. The candidate compounds produced calculated apparent association energies (E_{assn}) that ranged from −7.5 to −15.7 kcal/mol. The 13 best analogues, having apparent association energies less than −10 kcal/mol, were selected for synthesis as our best candidate agonists [Figure 6 (top), compounds A-1 through A-13]. Nine compounds having similar size and lipophilicity, but having markedly higher calculated apparent association energies, were also synthesized as negative controls [Figure 6 (bottom), compounds C-1 through C-9].

2.3. Transactivation Analysis of Biaryl Ligands in R274L. The members of the computationally focused library of bisphenol analogues were screened for their ability to induce ligand-dependent transcription response in HEK293 cells transiently transfected with pSG5VDR(R274L) and a vitamin D-responsive luciferase reporter by a standard dual luciferase reporter gene assay. The focused library was initially screened at two concentrations, 500 and 2000 nM, and the activities were compared to those obtained with $1,25(OH)_2D_3$ in VDR(wt). Activities are reported in relative light units (RLU), where the maximal inducible activity of VDR(wt) with $1,25(OH)_2D_3$ is set to 100 RLU.[38] Compounds having activities in VDR(R274L) greater than 60 RLU at 500 nM were defined as potential leads and were further analyzed in the mutant.

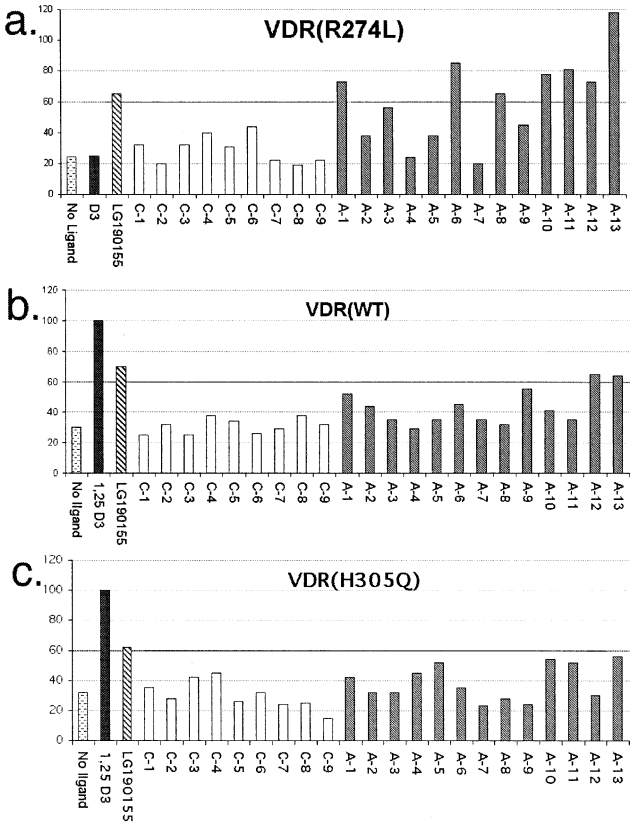

Figure 7. Cell-based screening of LG190155 analogues at 500 nM in (a) VDR(R274L), (b) VDR(wt), and (c) VDR(H305Q).

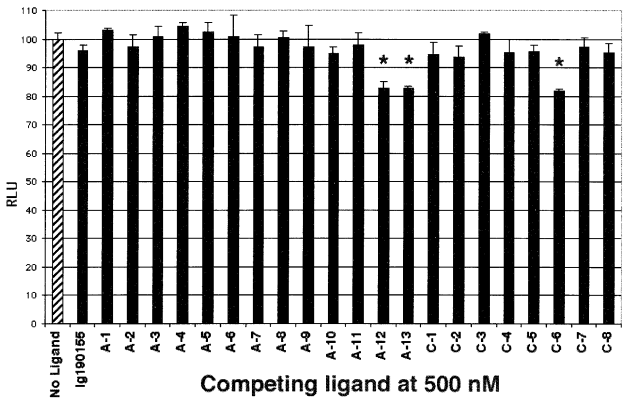

Figure 8. Cell-based screening of analogues for antagonist activity with VDR(wt). Luciferase reporter gene activity of HEK293 cells transiently expressing VDR(wt) in the presence of 100 nM $1,25(OH)_2D_3$ and 500 nM of each analogue. Asterisks indicate statistically significant difference (95%) from no competing ligand.

Initial screens of the 22-compound library identified seven analogues, A-1, A-6, A-8, A-10, A-11, A-12 and A-13, as potential leads for VDR(R274L) complementation (Figure 7a). By our selection criteria, more than half (7 of 13) of the designed analogues were identified as promising leads showing greater activity than LG190155, whereas none of the structurally similar

(38) Relative light units, RLU, are measured as the ratio of inducible firefly luciferase luminescence divided by the luminescence of the renilla luciferase control.

Table 1. Initial Screen and Molecular Modeling of Bisphenol Analogues in VDR(R274L)

ligand	receptor	RLU*a* (500 nM)	RLU*a* (2 μM)	Eassn (kcal)	EC50 (nM)	max RLU*b*	ligand	receptor	RLU*a* (500 nM)	RLU*a* (2 μM)	Eassn (kcal/mol)	EC50 (nM)	max RLU*b*
1,25(OH)2D 3	VDR*c*	100	100	8.8	2.1	100	A-1	R274 L	73	75	12.0	35. 7	79
LG190155	VDR*c*	58	82	9.0	110	88	A-2	R274 L	38	10.4	10.5		
1,25(OH)2D 3	R274 L	25	35	7.3	> 2000		A-3	R274 L	56	30	10.6		
LG190155	R274 L	62	80	9.5	85	62	A-4	R274 L	24	69	10.4		
C-1	R274 L	32	53	9.37			A-5	R274 L	38	40	10.4		
C-2	R274 L	20	21	8.7			A-6	R274 L	85	119	11.8	121	119
C-3	R274 L	32	32	8.47			A-7	R274 L	20	60	10.1		
C-4	R274 L	40	53	9.6			A-8	R274 L	65	68	10.1	8.07	63
C-5	R274 L	31	51	8.4			A-9	R274 L	45	70	15.7		
C-6	R274 L	44	57	8.4			A-10	R274 L	78	81	10.7	8.4	80
C-7	R274 L	22	52	9.4			A-11	R274 L	81	85	12.3	15.7	81
C-8	R274 L	19	31	8.4			A-12	R274 L	73	62	10.9	35.3	69
C-9	R274 L	22	30	7.5			A-13	R274 L	118	120	11.8	3.3	118

[a] RLU = relative light unit derived from cellular luciferase reporter gene assay. Background activity measured in the absence of ligand = 24 RLU. [b] Relative maximum activity = [RLU_{max}(analogue in VDR(R274L))]/[RLU_{max}[1,25$(OH)_2D_3$ in VDR(wt)]. Wild type.

control compounds was selected. In contrast, screening of the focused library in VDR(wt) identified only two analogues (A-11 and A-13) that had slightly greater than 60% the activity of 1,25$(OH)_2D_3$. The analogues A-12, A-13, and C-6 showed significant, but weak, antagonist activity at 500 nM with VDR(wt) in the presence of 100 nM 1,25$(OH)_2D_3$, suggesting that A-12 and A-13 are weak partial agonist/antagonists and C-6 is a weak antagonist (Figure 8). Furthermore, the unique c-2 symmetry of LG190155 suggests that our analogues could potentially be used to complement mutants such as VDR(H305Q), which is located on the opposite end of the pocket from Arg274, by binding in the opposite orientation. None of the analogues showed significant activity with the VDR(H305Q) mutant, supporting the notion that the activities observed with VDR(R274L) were by design (Figure 7b,c).

One does not necessarily predict a one-to-one correlation between the calculated E_{assn} and transcriptional activity; however, it is intriguing that the seven most active compounds were among the 10 compounds with the best (most negative E_{assn}) calculated association energies (Table 1). Together, these results indicate that binding-site models based on the agonized structure of NHRs can provide a powerful tool to exclude inactive compounds and to identify analogues that have a significant proclivity for being active agonists.

2.4. Rationally Designed Analogues Are Potent and Highly Active hVDR(R274L) Agonists. The full dose−response behavior of our identified leads A-1, A-6, A-8, A-10, A-11, A-12, and A-13 were evaluated in cellular reporter gene assays along with LG190155 in 1,25$(OH)_2D_3$ (Figure 9). Interestingly, LG190155 itself is a fairly potent agonist for VDR(R274L) (EC_{50} = 60 nM) and is more potent in the mutant receptor than in VDR(wt) [EC_{50}(wt) = 110 nM), which is consistent with our models. Of the seven active leads, six were very potent agonists in VDR(R274L), having EC_{50} values 2−25 times more potent than the parent compound LG190155 and greater than 16−526 times more potent than the natural ligand 1,25$(OH)_2D_3$. Six of the seven analogues show 2−18 times greater relative transcriptional potency in VDR(R274L) than JK-1626-2, a compound previously identified through screening of known 1,25$(OH)_2D_3$ analogues.[3] Six of the seven analogues also have greater maximally inducible activities than LG190155 in VDR(R274L). Significantly, three of the analogues represent highly active agonists for the mutant VDR(R274L) and are able to induce activities in the mutant that are similar to or even

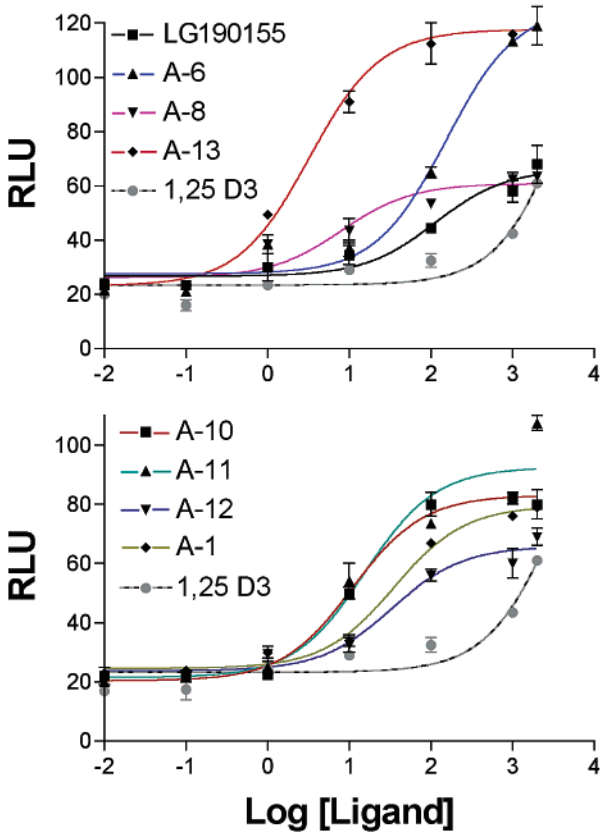

Figure 9. Dose−response behavior of lead compounds with VDR(R274L) in cellular reporter gene assays.

greater than that obtained with 1,25$(OH)_2D_3$ in VDR(wt). These results clearly support structure-based design as a rapid means to identify both potent and highly active agonists to otherwise mutationally impaired receptors.

2.5. Calcium Influx Activity of R274L Agonists Shows Selectivity against Membrane-Associated VDR and Overall Reduced Calcemic Effects. The generation of novel ligands capable of restoring activity to mutationally impaired receptors with high potency and selectivity represents an important first step toward the development of new therapies based on complementing genetic mutations with small molecules. As is the case with other hormone receptors associated with genetic disease, the mutant nuclear receptor often is not the only molecular target for the natural hormone. For this reason, the

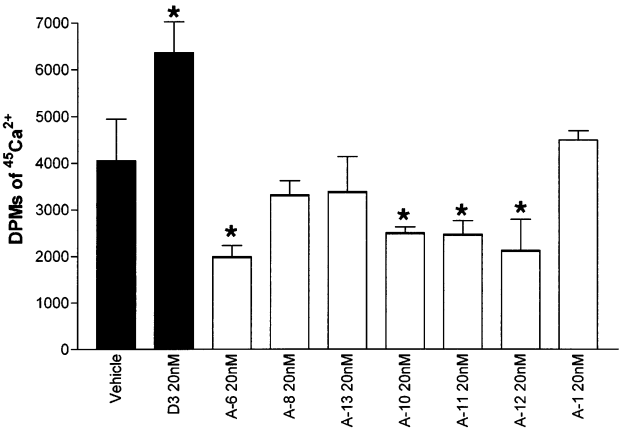

Figure 10. Stimulation of $^{45}Ca^{2+}$ influx of MC3T3-E1 preosteoblastic cells under stimulating conditions. D3 = $1,25(OH)_2D_3$. Error bars reflect 1 standard deviation of three independent experiments. Asterisks indicate statistically significant difference from vehicle at 95% confidence.

use of high doses of the natural hormone to activate a refractory receptor is generally undesirable because of the side effects associated with overstimulation of other endogenous receptors responsive to the same hormone. In the case of the homozygous mutations associated with rickets, one needs to avoid overstimulation of the membrane-associated $1,25(OH)_2D3$ receptor, which regulates rapid calcium transport across the cell membrane in various cell types.

To ascertain if our designed analogues stimulate $^{45}Ca^{2+}$ flux across the plasma membrane of a common target cell possessing the membrane-associated VDR, the lead compounds were evaluated in a standard cellular calcium influx assay.[39] Under depolarizing conditions (high external K^+), 20 nM $1,25(OH)_2D_3$ induced a 50% increase in $^{45}Ca^{2+}$ influx compared to vehicle control, whereas none of the seven leads at similar concentrations induced a significant increase in $^{45}Ca^{2+}$ influx (Figure 10). Similar results were observed when the assay was performed in normal K^+ (nondepolarizing) resting buffer (data not shown). These results show that the designed analogues can selectively restore activity to the mutant nuclear VDR(R274L) without triggering the rapid, membrane-initiated calcium responses associated with $1,25(OH)_2D_3$ and closely related analogues.

Structural biology is providing a unique opportunity to examine the molecular basis for many genetic diseases. In some instances, when mutations affect the association of small molecule ligands (or substrates), it is sometimes possible for appropriate small-molecule analogues to restore function to mutationally impaired proteins. These mutant proteins present a unique chemical challenge both to understand the molecular manifestations of the defect and to potentially design mutant-complementing analogues. Clearly, not all mutations can be "pharmacologically rescued" by small molecules; however, appropriate structural analogues may ultimately provide new approaches for the treatment of patients harboring a significant subset of these mutations.

The general observation that very few individuals may harbor any specific mutation emphasizes the need to be able to rapidly identify mutant-specific complements. In this study, structure-based design successfully identified several promising compounds based on a lead compound originally discovered to activate the wild-type receptor. Molecular modeling successfully provided a rapid means to identify analogues that had a significant likelihood to be potent and active agonists of the VDRR-associated mutant VDR(R274L) and was very efficient at identifying structurally similar analogues that were not likely to be active agonists. The best designed compounds were more potent, more active, and more selective than an analogue previously identified by screening of known $1,25(OH)_2D_3$ analogues.

Experimental Section

General. All compounds were purchased from Aldrich Chemical Co. (Milwaukee, WI) unless otherwise noted. NMR spectra were carried out on Bruker AM 250 and 600 MHz spectrophotometers at the University of Delaware NMR facility; chemical shifts are reported downfield from that of internal tetramethylsilane (TMS). Mass spectrophotometry was performed at the University of Delaware mass spectrometry laboratory. Custom oligonucleotides were purchased from Ranson Hill Bioscience Inc. HEK 293 cells were obtained from ATTC (American Type Tissue Collection) and were maintained at the University of Delaware cell culture core facility.

Cell Culture. All cell culture experiments were performed with Dulbecco's modified Eagle's medium (DMEM). Twenty-four hours prior to transfection, HEK293 cells were seeded at a density of 40×10^3 cells/well in 24-well culture plates. Three hours prior to transfection, the medium was changed to DMEM containing 10% charcoal-resin-stripped FBS (fetal bovine serum). Transfections were performed by the $CaPO_4$ method with 0.03 μg of VDRE-LUC, 0.14 μg of Renilla-Luc internal standard, and 0.08 μg of VDR per well Six hours after transfection, the medium was removed and replaced with DMEM with 10% charcoal-resin-stripped FBS containing appropriate concentrations of ligand. The cells were allowed to incubate for 36 h before being harvested by passive lysis. Cell extracts were immediately assayed by the dual-luciferase assay (Promega) with a Perkin-Elmer Microbeta luminometer. Activity is reported in relative light units (RLU), determined as the ratio of the inducible firefly luciferase luminescence divided by the luminescence of the renilla luciferase control. Dose−response data were analyzed by nonlinear regression analysis with Graphpad Prism.

Calcium influx assays were performed with MC3T3-E1 cells that were cultured as previously described.[39,40] Cells were seeded at a density of 50000 cells/mL onto 3.5-cm dishes and grown to approximately 50% confluency. Culture medium was aspirated, and the cells were washed with depolarizing buffer (5 mM NaCl, 132 mM KCl, 1.3 mM $MgCl_2$, 1.2 mM $CaCl_2$, 10 mM d-glucose, and 25 mM Tris-HCl, pH 7.4). Then the cells were incubated for 2 min with room-temperature buffer, resting buffer plus 1 nM $1,25(OH)_2D_3$, or analogue. All solutions contained 12.5 μCi/mL $45Ca^{2+}$ (NEN Life Science Products). Uptake was terminated by aspiration of the labeling solution followed by three washes with ice-cold resting buffer. Cell-associated $^{45}Ca^{2+}$ was measured by extraction with 0.5 N NaOH and liquid scintillation counting.[41]

Plasmid Constructs. Mammalian expression vectors pSG5-HVDR(R274L) and pSG5-HVDR(H305Q) were constructed from parent plasmid pSG5-HVDR(wt) (kindly provided by Dr. Mark Haussler, University of Arizona) by oligonucleotide-directed mutagenesis with Quickchange (Stratagene) and the following nucleotides:

*h*VDR(H305Q);gtgaccaaagccggacagagcctggagctg, cagctccaggctctgtcc-ggctttggtcac. *h*VDR(R274L); gccattgaggtcatcatgttgctgtccaatgagtccttcac, gtgaaggactcattggacagcaacatgatgacctcaatggc.

(39) Meszaros, J. G.; Farach-Carson, M. C. *Methods Enzymol.* **1999**, *282*, 236−243.

(40) Meszaros, J. G.; Karin, N. J.; Farach-Carson, M. C. *Connect. Tissue Res.* **1996**, *35*, 107−11.

(41) Liu, R.; Li, W.; Karin, N. J.; Bergh, J. J.; Adler-Storthz, K.; Farach-Carson, M. C. *J. Biol. Chem.* **2000**, *275*, 8711−1718.

All constructs were sequenced over the entire coding region of the VDR to confirm the presence of only the desired mutation. VDRE-luc contains the firefly luciferase gene located downstream of the vitamin D-responsive human osteopontin promoter.[42]

Syntheses. The syntheses of intermediate **3** and analogues **A-1** to **A-13** and **C-1** to **C-9** are described below. The synthesis of 3,3-bis-(3-methyl-4-hydroxyphenyl)pentane (**1**) and 3,3-bis[4-(2-oxo-3,3-dimethylbutoxy)-3-methylphenyl)]pentane (**2**) has been previously reported by Boehm et al.[22]

3-[4-(2-Oxo-3,3-dimethylbutoxy)-3-methylphenyl)]-3-[4-(4_-vinylbenzyloxy)-3-methylphenyl]pentane (3). To 100 mg (0.29 mmol) of **2** in 1.4 mL of DMF was added 15 mg (0.38 mmol) of NaH. The mixture was stirred at room temperature for 30 min before 0.085 mL (0.39 mmol) of 4-vinylbenzyl chloride was added. The reaction was stirred for an additional 30 min before 2 mL of H_2O and 4 mL of EtOAc were added. The organic layer was separated and washed with 2 mL of brine, dried over $MgSO_4$, and concentrated under reduced pressure. Purification by flash silica chromatography (10% EtOAc/hexanes) yielded 103 mg (72%) of **3** as a colorless oil. ^{1}H NMR (250 MHz) δ 0.62 (t, J = 7.0 Hz, 6H), 1.27 (s, 9H), 2.05 (q, J = 7.0 Hz, 4H), 2.25 (s, 3H), 2.27 (s, 3H), 4.85 (s, 2H), 5.05 (s, 2H), 5.27, (d, J = 8.25 Hz, 1H), 5.77 (d, J = 17.5 Hz, 1H), 6.53 (d, J = 8.25 Hz, 1H), 6.80 (m, 2H), 7.0, (m, 4H), 7.5 (m, 4H); ^{13}C NMR (400 MHz) δ 8.9, 17.2, 26.8, 43.7, 48.8, 69.9, 70.0, 110.51, 110.6, 114.3, 126.2, 126.3, 126.5, 126.7, 127.8, 131, 131.1, 136.9, 137.4, 137.7, 141.3, 142.0, 154.3, 154.9, 210.6; MS (ES) calculated for $C_{34}H_{42}NaO_3$ 521.37, found 521.3 (M + Na).

3-[4-(2-Oxo-3,3-dimethylbutoxy)-3-methylphenyl)]-3-[4-(4′-formylbenzyloxy)-3-methylphenyl]pentane (A-1). A nitrogen-purged solution of 20 mg (0.04 mmol) of **3** in 1 mL of CH_2Cl_2 and 0.01 mL of pyridine was charged with a stream of O_3 for 30 s. The solution was then purged with N_2 for 30 s and quenched by addition of 0.025 mL (0.4 mmol) of DMS. The reaction was warmed to room temperature and concentrated under reduced pressure. The oily residue was dissolved in 2 mL of EtOAc, washed 2 × 1 mL with brine, and dried over $MgSO_4$. Purification by flash silica chromatography (10% EtOAc/hexanes) afforded 13 mg (65%) of **A-14** as a colorless oil. ^{1}H NMR (250 MHz) δ 0.58 (t, J = 7.5 Hz, 6H), 1.26 (s, 9H), 2.02 (q, J = 7.5 Hz, 4H), 2.25 (s, 6H), 4.87 (s, 2H), 5.13 (s, 2H), 6.5 (d, J = 8.5 Hz, 1H), 6.75 (d, J = 8.5 Hz, 1H), 6.87−7.01 (m, 4H), 7.7 (d, J = 8.3 Hz, 2H), 7.9 (d, J = 8.3 Hz, 2H), 10.1, (s, 1H); ^{13}C NMR (400 MHz) δ 8.9, 17.1, 26.8, 29.6, 43.7, 48.8, 69.4, 69.9, 110.4, 110.5, 126.1, 126.4, 126.5, 126.6, 127.6, 130.4, 131.2, 136.2, 141.7, 141.9, 145.2, 154.4, 154.5, 192.5, 210.6; MS (ES) calculated for $^{C}{}_{33}H_{40}O_4Na$ 523.36, found 523.3 (M + Na).

3-[4-(2-Hydroxy-3,3-dimethylbutoxy)-3-methylphenyl)]-3-[4-(3-phenoxypropoxy)-3-methyl phenyl]pentane (A-2). To a 0 °C solution of 10 mg of **A-5** (0.020 mmol) in 0.11 mL of MeOH was added 2 mg (0.046 mmol) of $NaBH_4$. This mixture was stirred at 0 °C for 30 min before 2 mL of NH_4Cl and 3 mL of EtOAc were added. The organic layer was separated and washed with 1 mL of brine, dried over $MgSO_4$, and concentrated under reduced pressure. Purification by flash silica chromatography (10% EtOAc/hexanes) yielded 7 mg (70%) of **A-2** as a colorless oil. ^{1}H NMR (250 MHz) δ 0.58 (t, J = 7 Hz, 6H), 1.0 (s, 9H), 2.03 (q, J = 7 Hz, 4H), 2.2, (s, 3H), 2.22 (s, 3H), 2.25−2.3 (m, 2H), 2.5 (br s, 1H), 3.75 (m, 1H), 3.80, (t, J = 8.2 Hz, 1H), 4.08−4.25 (m, 5H), 6.7−6.75 (m, 2H), 6.85−7.02 (m, 6H), 7.25−7.35 (m, 3H); $_{13}$C NMR (400 MHz) δ 8.9, 17.0, 26.5, 29.7, 29.9, 48.8, 64.6, 64.9, 69.6, 77.7, 107.9, 110.2, 110.5, 114.9, 121.1, 125.9, 126.5, 126.6, 129.9, 131.0, 131.1, 141.0, 141.7, 154.7, 155.0, 159.3; MS (ES) calculated for $C_{34}H_{46}O_4Na$ 541.37, found 541.3 (M + Na).

3-[4-(2-Oxo-3,3-dimethylbutoxy)-3-methylphenyl)]-3-[4-(4-hydroxy-4-methylpentoxy)-3-me thylphenyl]pentane (A-3). To a solution of 20 mg (0.080 mmol) of **1** in 0.26 mL of DMF was added 2.5 mg (0.104 mmol) of NaH. This mixture was stirred at room temperature for 30 min before 0.014 mL (0.080 mmol) of 4-bromo-phenylpropane and 0.012 mL (0.080 mmol) of 3-methyl-3-trimethylsiloxy-1-chlorobutane were added.[43] The reaction was stirred for an additional 30 min before addition of 2 mL of H_2O and 3 mL of EtOAc. The organic layer was washed with 1 mL of brine, dried over $MgSO_4$, and concentrated under reduced pressure. Purification by flash silica chromatography (20% EtOAc/hexanes) yielded 4 mg (10%) of **A-3** as a colorless oil. ^{1}H NMR (250 MHz) δ 0.62 (t, J = 7.5 Hz, 6H), 1.36 (s, 9H), 2.1 (m, 4H), 2.2, (m, 2H), 2.25 (s, 3H), 2.27 (s, 3H), 2.8 (t, J = 6.5 Hz, 2H), 3.98 (t, J = 6.5 Hz, 2H), 4.22 (t, J = 6.5 Hz, 2H), 6.71 (d, J = 8.3 Hz, 1H), 6.75 (d, J = 8.3 Hz, 1H), 6.87−7.14 (m, 4H), 7.2−7.45 (m, 5H); ^{13}C NMR (400 MHz) δ 8.9, 17.0, 17.3,, 29.7, 29.8, 31.5, 32.8,41.9, 48.8, 65.5, 67.1, 71.0, 109.9, 110.1, 125.5, 125.9, 126.3, 126.4, 126.6, 128.8, 128.9, 130.8, 131.0, 140.8, 141.6, 142.2, 154.6, 155.1; MS (ES) calculated for $C_{33}H_{44}O_3Na$ 511.36, found 511.3 (M + Na).

3-[4-(2-Oxo-3,3-dimethylbutoxy)-3-methylphenyl)]-3-[4-(2-phenyl-2-oxoethoxy)-3-methylphenyl]pentane (A-4). To a solution of 20 mg (0.057 mmol) of **2** in 0.26 mL of DMF was added 3 mg (0.078 mmol) of NaH. The mixture was stirred at room temperature for 30 min before 0.014 mL (0.068 mmol) of 2-bromoacetophenone was added. The reaction was stirred for an additional 30 min before 2 mL of H_2O and 3 mL of EtOAc were added. The organic layer was washed with 1 mL of brine, dried over $MgSO_4$, and concentrated under reduced pressure. Purification by flash silica chromatography (10% EtOAc/hexanes) afforded 12 mg (42%) of **A-4** as a colorless oil. ^{1}H NMR (250 MHz) δ 0.65 (t, J = 7.0 Hz, 6H), 1.25 (s, 9H), 2.0 (q, J = 7.0 Hz, 4H), 2.25 (s, 3H), 2.26 (s, 3H), 4.8 (s, 2H), 5.25 (s, 2H), 6.5 (d, J = 8.3 Hz, 1H), 6.63 (d, J = 8.3 Hz, 1H), 6.8−7.0 (m, 4H), 7.5−7.7 (m, 3H), 8.0 (d, J = 8.5 Hz, 2H); ^{13}C NMR (400 MHz) δ 8.5, 16.6, 26.4, 29.2, 43.2, 48.4, 69.6, 71.2, 110.1, 110.3, 125.9, 126.0, 126.1, 128.2, 128.7, 130.7, 130.8, 133.7, 134.7, 141.4, 141.6, 153.8, 153.9, 195.2, 210.1; MS (ES) calculated for $C_{33}H_{40}O_4Na$ 523.36, found 523.2 (M + Na).

3-[4-(2-Oxo-3,3-dimethylbutoxy)-3-methylphenyl)]-3-[4-(3-phenoxypropoxy)-3-methylphenyl] pentane (A-5). To a solution of 20 mg (0.057 mmol) of **2** in 0.26 mL of DMF was added 3 mg (0.078 mmol) of NaH. This mixture was stirred at room temperature for 30 min before 0.014 mL (0.068 mmol) of 4-bromophenoxypropane was added. The reaction was stirred for an additional 30 min before 2 mL of H_2O and 3 mL of EtOAc were added. The organic layer was partitioned, washed with 1 mL of brine, dried over $MgSO_4$, and concentrated under reduced pressure. Purification by flash silica chromatography (10% EtOAc/hexanes) afforded 17 mg (56%) of **A-5** as a colorless oil. ^{1}H NMR (250 MHz) δ 0.53 (t, J = 7.5 Hz, 6H), 1.27 (s, 9H), 2.0 (q, J = 7.5 Hz, 4H), 2.13, (s, 3H), 2.18−2.30 (m, 5H), 4.05−4.25 (m, 4H), 4.8 (s, 2H), 6.5 (d, J = 8.3 Hz, 1H), 6.75 (d, J = 8.3 Hz, 1H), 6.8−7.0 (m, 6H), 7.2−7.35 (m, 3H); ^{13}C NMR (250 MHz) δ 8.9, 15.8, 29.8, 31.5, 32.2, 43.7, 48.8, 64.7, 65.1, 67.4, 109.9, 110.2, 111.4, 117.3, 124.2, 125.0, 125.2, 130.2, 132.3, 132.5, 140.0, 140.5, 153.1, 155.3, 159.8, 209.3; MS (ES) calculated for $C_{34}H_{44}O_4Na$ 539.37, found 539.3 (M + Na).

3-[4-(2-Hydroxy-3,3-dimethylbutoxy)-3-methylphenyl)]-3-[4-(4-(hydroxymethyl)benzyloxy)-3 -methylphenyl]pentane (A-6). To a 0 °C solution of 10 mg of **A-14** (0.020 mmol) in 0.11 mL of MeOH was added 2 mg (0.046 mmol) of NaBH4. The mixture was stirred at 0 °C for 30 min before 2 mL of NH_4Cl and 3 mL of EtOAc were added. The organic layer was washed with 1 mL of brine, dried over $MgSO_4$, and concentrated in vacuo. Purification by silica flash chromatography (25% EtOAc/hexanes) afforded 8 mg (79%) of **A-6** as a colorless oil. ^{1}H NMR (250 MHz) δ 0.58 (t, J = 7.5 Hz, 6H), 1.02 (s, 9H), 1.8−2.05 (m, 4H), 2.2, (s, 3H), 2.25 (s, 3H), 2.5 (br s, 1H), 3.67−4.13 (m,

(42) Yamamoto, S.; Hijiya, N.; Setoguchi, M.; Matsuura, K.; Ishida, T.; Higuchi, Y.; Akizuki, S. *Ann. N.Y. Acad. Sci*. **1995**, *760*, 44−58.

(43) Andrews, D. R.; Barton, D. H. R.; Hesse, R. H.; Pechet, M. M. *J. Org. Chem*. **1986**, *51*, 4819−4828.

3H), 4.75 (s, 2H) 5.0 (s, 2H), 6.73 (d, $J = 8.3$ Hz, 1H), 6.75 (d, $J = 8.3$ Hz, 1H), 6.78−7.0 (m, 4H), 7.25−7.5 (m, 4H); ^{13}C NMR (400 MHz) δ 8.7, 16.9, 26.3, 29.4, 33.8, 48.6, 65.4, 69.3, 69.7, 77.2, 110.2, 110.4, 125.6, 125.9, 126.2, 126.3, 127.4, 127.6, 130.8, 130.9, 137.4, 140.5, 141.1, 141.4, 154.2, 154.4, 154.5; MS (ES) calculated for $C_{33}H_{44}O_4Na$ 527.36, found 527.0 (M + Na).

3-[4-(2-Hydroxy-3,3-dimethylbutoxy)-3-methylphenyl)]-3-[4-(3-phenylpropoxy)-3-methylphenyl]pentane (A-7). To a 0 °C solution of 10 mg (0.020 mmol) of **A-8** in 0.1 mL of MeOH was added 1.0 mg (0.026 mmol) of $NaBH_4$. The mixture was stirred at 0 °C for 30 min before 2 mL of NH_4Cl and 3 mL of EtOAc were added. The organic layer was washed with 1 mL of brine, dried over $MgSO_4$, and concentrated under reduced pressure. Purification by flash silica chromatography (10% EtOAc/hexanes) yielded 6 mg (60%) of **A-7** as a colorless oil. ^{1}H NMR (250 MHz) δ 0.58 (t, $J = 7.5$ Hz, 6H), 1.0 (s, 9H), 2.0−2.23 (m, 6H), 2.2, (s, 3H), 2.24 (s, 3H), 2.5, (br s, 1H), 2.8 (t, $J = 6.5$ Hz, 2H), 3.7−4.2 (m, 5H), 6.62−6.75 (m, 2H), 6.85−7.10 (m, 4H), 7.12−7.40 (m, 5H); ^{13}C NMR (250 MHz) δ 8.7, 17.1, 26.2, 29.5, 31.3, 32.5, 33.7, 48.5, 66.9, 69.2, 76.9, 109.9, 110.2, 125.5, 125.6, 126.0, 126.1, 128.4, 128.7, 130.4, 130.6, 130.9, 140.5, 141.4, 141.9, 154.4, 154.8; MS (ES) calculated for $C_{34}H_{46}O_3Na$ 525.37, found 525.3 (M + Na).

3-[4-(2-Oxo-3,3-dimethylbutoxy)-3-methylphenyl)]-3-[4-(3-phenylpropoxy)-3-methylphenyl]pentane (A-8). To a solution of 20 mg (0.057 mmol) of **2** in 0.26 mL of DMF was added 3 mg (0.078 mmol) of NaH. The mixture was stirred at room temperature for 30 min before 0.014 mL (0.068 mmol) of 4-bromophenylpropane was added. After 30 min, 2 mL of H_2O and 3 mL of EtOAc were added. The organic layer was washed with 1 mL of brine, dried over $MgSO_4$, and concentrated under reduced pressure. Purification by flash silica chromatography (10% EtOAc/hexanes) afforded 17 mg (64%) of **A-8** as a colorless oil. ^{1}H NMR (250 MHz) δ 0.58 (t, $J = 7.5$ Hz, 6H), 1.23 (s, 9H), 2.1 (q, $J = 7.5$ Hz, 4H), 2.0−2.2, (m, 2H), 2.25 (s, 3H), 2.28 (s, 3H), 2.8 (t, $J = 6.5$ Hz, 2H), 3.98 (t, $J = 6.5$ Hz, 2H), 4.8 (s, 2H), 6.5 (d, $J = 8.5$ Hz, 1H), 6.68 (d, $J = 8.5$ Hz, 1H), 6.95 (m, 4H), 7.1−7.4 (m, 5H); ^{13}C NMR (400 MHz): δ 8.9, 17.1, 26.8, 29.7, 31.6, 32.8, 43.7,48.8, 67.1, 70.0, 110.1, 110.5, 125.9, 126.2, 126.3, 126.5, 128.8, 128.9, 130.9, 131.2, 140.8, 142.1, 142.2, 154.3, 155.1, 210.6; MS (ES) calculated for $C_{34}H_{44}O_3Na$ 523.37, found 523.3 (M + Na).

3-[4-(2-Oxo-3,3-dimethylbutoxy)-3-methylphenyl)]-3-[4-(4-carboxybenzyloxy)-3-methylphenyl]pentane (A-9). To a solution of 20 mg (0.057 mmol) of **2** in 0.26 mL of DMF was added 3 mg (0.078 mmol) of NaH. The mixture was stirred at room temperature for 30 min before 0.016 mg (0.068 mmol) of α-bromomethyltoluate was added.[44] The reaction was stirred for an additional 30 min before 2 mL of H_2O and 3 mL of EtOAc were added. The organic layer was washed with 1 mL of brine, dried over $MgSO_4$, and concentrated under reduced pressure. The oily residue was dissolved in 0.3 mL of EtOH and treated with 0.010 mL of 3 M NaOH. The solution was refluxed for 2 h and then cooled before 2 mL of 1 N HCl and 3 mL of EtOAc were added. Purification by flash silica chromatography (40% EtOAc/hexanes) afforded 8 mg (28%) of **A-9** as a colorless oil. ^{1}H NMR (250 MHz) δ 0.63 (t, $J = 7.5$ Hz, 6H), 1.30 (s, 9H), 2.07 (q, $J = 7.5$ Hz, 4H), 2.28, (s, 6H), 4.82 (s, 2H), 5.2 (s, 2H), 6.52 (d, $J = 8.5$ Hz, 1H), 6.75 (d, $J = 8.5$ Hz, 1H), 6.8−7.08 (m, 4H), 7.6, (d, $J = 8.3$, 2H), 8.2 (d, $J = 8.3$ Hz, 2H); ^{13}C NMR (400 MHz) δ 8.9, 17.1, 26.8, 27.1, 29.7, 48.8, 69.5, 70.0, 110.5, 110.6, 116.2, 124.4, 126.1, 126.2, 126.5, 129.0, 131.1, 131.2, 141.6, 141.9, 152.1, 186.2, 210.0; MS (ES) calculated for $C_{33}H_{40}O_5Na$ 539.36, found 539.2 (M + Na).

3-[4-(2-Oxo-3,3-dimethylbutoxy)-3-methylphenyl)]-3-[4-(2-((2-tetrahydropyranyl)oxy)ethoxy)-3-methylphenyl]pentane (A-10). To a solution of 20 mg of **2** (0.052 mmol) in 0.26 mL of DMF was added 3 mg (0.078 mmol) of NaH. The mixture was stirred at room temperature for 30 min before 0.0125 mL (0.0688 mmol) of 2-(2-bromoethoxy)tetrahydro-2*H*-pyran. The reaction was stirred for an additional 30 min before 2 mL of H_2O and 3 mL of EtOAc were added. The organic layer was separated, washed with 1 mL of brine, dried over $MgSO_4$, and concentrated under reduced pressure. Purification by flash silica chromatography (10% EtOAc/hexanes) afforded 15 mg (58%) of **A-10** as a colorless oil. ^{1}H NMR (250 MHz) δ 0.58 (t, $J = 7.5$ Hz, 6H), 1.25 (s, 9H), 1.48−1.95 (m 6H), 2.0 (q, $J = 7.5$ Hz, 4H), 2.21 (s, 3H), 2.25 (s, 3H), 3.5−4.2 (m, 6H), 4.72−4.77 (m, 1H), 4.8 (s, 2H), 6.5 (d, $J = 8.5$ Hz, 1H), 6.72 (d, $J = 8.5$ Hz, 1H), 6.95−7.02 (m, 4H); ^{13}C NMR (400 MHz) δ 8.9, 17.0, 19.7, 25.9, 26.8, 29.7, 30.9, 43.7, 48.8, 62.4, 66.3, 67.8, 70.0, 99.3, 110.4, 110.5, 126.0, 126.3, 126.4, 126.5, 130.9, 131.2, 141.1, 142.0, 154.3, 155.0, 210.6; MS (ES) calculated for $C_{32}H_{46}O_5Na$ 533.35, found 533.4 (M + Na).

3-[4-(2-Oxo-3,3-dimethylbutoxy)-3-methylphenyl)]-3-[4-(4′-(hydroxymethyl)benzyloxy)-3-methylphenyl]pentane (A-11). To a solution of 20 mg (0.043 mmol) of **A-14** in 0.3 mL of CH_2Cl_2 at 0 °C was added 2.5 mg (0.028 mmol) of *t*-butylamine−borane compex. This solution was stirred at 0 °C for 10 min before 1 mL of 2 N HCl was added. The reaction mixture was vigorously stirred for 20 min at room temperature and then diluted with 3 mL of EtOAc. The organic layer was washed with 1 mL of NaHCO3 (saturated) and 1 mL of brine and then dried over $MgSO_4$. Purification by flash silica chromatography (10%EtOAc/Hexanes) afforded 13 mg (65%) of **A-11** as a colorless oil. ^{1}H NMR (250 MHz) δ 0.62 (t, $J = 7.5$ Hz, 6H), 1.25 (s, 9H), 2.1 (q, $J = 7.5$ Hz, 4H), 2.23 (s, 3H), 2.26 (s, 3H), 4.75 (s, 2H), 4.82 (s, 2H), 5.07 (s, 2H), 6.53 (d, $J = 8.5$ Hz, 1H), 6.78 (d, $J = 8.5$ Hz, 1H), 6.85−7.0 (m, 4H), 7.47 (q, $J = 8.25$ Hz, 4H); ^{13}C NMR (400 MHz) δ 8.7, 16.9, 26.6, 29.4, 48.6, 65.4, 69.7, 69.8, 110.3, 110.4, 125.9, 126.1, 126.2, 126.3, 127.4, 127.6, 130.8, 131.0, 137.4, 140.5, 141.1, 141.8, 154.7, 210.4; MS (ES) calculated for $C_{33}H_{42}O_4Na$ 525.36, found 525.3 (M + Na).

3-[4-(2-Hydroxy-3,3-dimethylbutoxy)-3-methylphenyl)]-3-[4-(2-((2-tetrahydropyranyl)oxy)ethoxy)-3-methylphenyl]pentane (A-12). To a solution of 10 mg of **A-10** (0.021 mmol) in 0.26 mL of MeOH at 0 °C was added 1.6 mg (0.042 mmol) of NaBH4. The mixture was stirred at 0 °C for 30 min before 1 mL of NH4Cl and 3 mL of EtOAc was added. The organic layer was washed with 1 mL of brine, dried over $MgSO_4$, and concentrated under reduced pressure. Purification by flash silica chromatography (10% EtOAc/hexanes) afforded 8 mg (71%) of **A-12** as a colorless oil. ^{1}H NMR (250 MHz) δ 0.62 (t, $J = 7.5$ Hz, 6H), 1.05 (s, 9H), 1.48−1.95 (m, 6H), 2.06 (q, $J = 7.5$ Hz, 4H), 2.21, (s, 6H), 2.5 (m, 1H), 3.5−4.25 (m, 9H), 4.8 (m, 1H), 6.72 (d, $J = 8.5$ Hz, 1H), 6.75 (d, $J = 8.5$ Hz, 1H), 6.83−7.05 (m, 4H); ^{13}C NMR (400 MHz) δ 8.9, 17.0, 19.7, 25.9, 26.5, 29.6, 30.9, 40.0, 48.8, 62.4, 66.3, 67.8, 69.5, 77.8, 99.3, 110.4, 110.5, 126.1, 126.4, 126.5, 131.2, 131.4, 141.1, 142.1, 154.3, 155.0; MS (ES) calculated for $C_{32}H_{48}O_5Na$ 535.35, found 535.4 (M + Na).

3-[4-(2-Oxo-3,3-dimethylbutoxy)-3-methylphenyl)]-3-[4-(4′-acetylbenzyloxy)-3-methylphenyl]pentane (A-13). To a solution of 20 mg of **2** (0.052 mmol) in 0.26 mL of DMF was added 3 mg of NaH. The mixture was stirred at room temperature for 30 min before 0.012 mL (0.062 mmol) of 4′-acetylbenzylbromide was added.[45] The reaction was stirred for an additional 30 min before 2 mL of H_2O and 3 mL of EtOAc were added. The organic layer was washed with 1 mL of brine, dried over $MgSO_4$, and concentrated under reduced pressure. Purification by flash silica chromatography (10% EtOAc/hexanes) afforded 15 mg of **A-13** as a clear oil. ^{1}H NMR (250 MHz) δ 0.63 (t, $J = 7.5$ Hz, 6H), 1.27 (s, 9H), 2.06 (q, $J = 7.5$ Hz, 4H), 2.28 (s, 6H), 2.7 (s, 3H), 4.8 (s, 2H), 5.15 (s, 2H), 6.53 (d, $J = 8.5$ Hz, 1H), 6.75 (d, $J = 8.5$ Hz, 1H), 6.78−7.1 (m, 4H), 7.6 (d, $J = 8.25$, 2H), 8.0 (d, $J = 8.25$ Hz, 2H); ^{13}C NMR (400 MHz) δ 8.9, 17.1, 26.8, 27.1, 29.7, 43.7, 48.8, 69.5, 70.0, 110.5, 126.1, 126.4, 126.5, 126.6, 127.1, 127.3, 127.6, 129.0,

(44) Kelley, J. L.; Linn, J. A.; Selway, J. W. T. *J. Med. Chem.* **1989**, *32*, 1757−1763.

(45) Summers, J. B.; Gunn, B. P.; Martin J. G.; Martin, M. B.; Mazdiyasni, H.; Stewart, A. O.; Young, P. R.; Bouski, J. B.; Goetze, A. M.; et al. *J. Med. Chem.* **1988**, *31*, 1960−1964.

131.1, 131.2, 136.8, 141.6, 141.9, 143.6, 154.4, 154.6, 198.3, 210.5; MS (ES) calculated for $C_{34}H_{42}O_4Na$ 537.37, found 537.3 (M + Na).

3-[4-(2-Hydroxy-3,3-dimethylbutoxy)-3-methylphenyl]-3-[4-(2-hydroxy-2-phenylethoxy)-3-methylphenyl]pentane (C-1). To a 0 °C solution of 10 mg of **C-2** (0.017 mmol) in 0.09 mL of MeOH was added 1.5 mg (0.04 mmol) of $NaBH_4$. The mixture was stirred at 0 °C for 30 min before 1 mL of NH_4Cl and 3 mL of EtOAc were added. The organic layer was separated, washed with 1 mL of brine, and dried over $MgSO_4$. Purification by flash silica chromatography (40% EtOAc/hexanes) afforded 6 mg (58%) of **C-1** as a colorless oil. ^{1}H NMR (400 MHz) δ 0.58 (t, J = 7.5 Hz, 6H), 1.00 (s, 9H), 2.00 (q, J = 7.5 Hz, 4H), 2.17 (s, 3H), 2.2 (s, 3H), 2.4 (s, 1H), 2.85 (s, 1H), 3.7 (m, 1H), 3.85 (t, J = 7 Hz, 1H), 4.0−4.2 (m, 3H), 5.15 (m, 1H), 6.7 (m, 2H), 6.8−7.0 (m, 4H), 7.3 (t, J = 8.5 Hz, 1H), 7.4 (t, J = 8.25 Hz, 2H), 7.52 (d, J = 8.25 Hz, 2H), 7.62 (t, J = 8.25 Hz, 4H); ^{13}C NMR (400 MHz) 8.4, 16.7, 26.4, 30.9, 43.2, 48.4, 69.7, 71.4, 98.2, 110.1, 110.2, 110.4, 125.9, 126.0, 126.1, 127.3, 127.4, 127.5, 128.4, 128.5, 128.9, 129.0, 129.6, 130.7, 130.8, 141.4, 141.6, 153.9; MS (ES) calculated for $C_{39}H_{48}O_4Na$ 603.43, found 603.28 (M + Na).

3-[4-(2-Oxo-3,3-dimethylbutoxy)-3-methylphenyl]-3-[4-(2-(4′-phenyl)phenyl-2-oxoethoxy)-3-methylphenyl]pentane (C-2). To a solution of 20 mg (0.057 mmol) of **2** in 0.26 mL of DMF was added 3 mg (0.078 mmol) of NaH. The mixture was stirred at room temperature for 30 min before 19 mg (0.068 mmol) of 4′-phenyl-2-bromoacetophenone was added. The reaction was stirred for an additional 30 min before 2 mL of H_2O and 3 mL of EtOAc were added. The organic layer was separated, washed with 1 mL of brine, and dried over $MgSO_4$. Purification by flash silica chromatography (25% EtOAc/hexanes) afforded 20 mg (61%) of **C-2** as a colorless oil. ^{1}H NMR (250 MHz) δ 0.58 (t, J = 7.5 Hz, 6H), 1.27 (s, 9H), 2.0 (q, J = 7.5 Hz, 4H), 2.25 (s, 6H), 4.8 (s, 2H), 5.25 (s, 2H), 6.5 (d, J = 8.5, 1H), 6.70 (d, J = 8.5 Hz, 1H), 6.75−7.0 (m, 4H), 7.3−7.5 (m, 3H), 7.62 (d, J = 8.3 Hz, 2H), 7.73 (d, J = 8.3 Hz, 2H), 8.07 (d, J = 8.3 Hz, 2H); ^{13}C NMR (400 MHz) δ 8.4, 16.7, 26.0, 29.2, 48.4, 33.5, 69.1, 72.5, 73.2, 77.3, 110.0, 110.1, 125.5, 126.1, 126.2, 126.8, 127.1, 127.3, 127.4, 128.8,,130.6, 130.7, 138.9, 140.7, 141.0, 141.1, 141.4, 154.0, 154.2; MS (ES) calculated for $C_{39}H_{44}O_4Na$ 599.43, found 599.3 (M + Na).

3-[4-(2-Oxo-3,3-dimethylbutoxy)-3-methylphenyl)]-3-[4-(4′-phenylbenzyloxy)-3-methylphenyl]pentane (C-3). To a solution of 20 mg (0.057 mmol) of **2** in 0.26 mL of DMF was added 3 mg (0.078 mmol) of NaH. The mixture was stirred at room temperature for 30 min before 0.014 g (0.068 mmol) of 4-phenylbenzyl chloride was added. The reaction was stirred for an additional 30 min before 2 mL of H_2O and 3 mL of EtOAc was added. The organic layer was washed with 1 mL of brine and dried over $MgSO_4$ and concentrated under reduced pressure. Purification by flash silica chromatography (10% EtOAc/hexanes) afforded 21 mg (67%) of **C-3** as a colorless oil. ^{1}H NMR (400 MHz) δ 0.52 (t, J = 7.5 Hz, 6H), 1.15 (s, 9H), 1.92 (q, J = 7.5 Hz, 4H), 2.15, (s, 6H), 4.72 (s, 2H), 5.0 (s, 2H), 6.45 (d, J = 8.5 Hz, 1H), 6.72 (d, J = 8.5 Hz, 1H), 6.8−6.95 (m, 4H), 7.25 (t, J = 8.3 Hz, 1H), 7.35 (t, J = 8.3 Hz, 2H), 7.4 (d, J = 8.3 Hz, 2H), 7.52 (d, J = 8.3 Hz, 4H); ^{13}C NMR (400 MHz):δ 8.9, 17.1, 26.7, 29.8, 44.1, 48.9, 68.9, 70.0, 110.6, 110.7, 124.2, 125.8, 126.2, 126.4, 126.5, 126.6, 129.0, 131.0, 131.2, 133.5, 141.3, 142.0, 154.4, 155.1, 210.6; MS (ES) calculated for $C_{38}H_{44}O_3Na$ 571.42, found 571.3 (M + Na).

3-[4-(2-Oxo-3,3-dimethylbutoxy)-3-methylphenyl)]-3-[4-(2-(4′-fluorophenyl)-2-oxoethoxy)-3-methylphenyl]pentane (C-4). To a solution of 20 mg (0.057 mmol) of **2** in 0.26 mL of DMF was added 3 mg (0.078 mmol) of NaH. The mixture was stirred at room temperature for 30 min before 15 mg (0.068 mmol) of 4′-fluoro-2-bromoacetophenone was added. The reaction was stirred for an additional 30 min before 2 mL of H_2O and 3 mL of EtOAc were added. The organic layer was washed with 1 mL of brine, dried over $MgSO_4$, and concentrated under reduced pressure. Purification by flash silica chromatography (10% EtOAc/hexanes) afforded 13 mg (44%) of **C-4** as a colorless oil. ^{1}H NMR (250 MHz) δ 0.58 (t, J = 7.5 Hz, 6H), 1.27 (s, 9H), 2.0 (q, J = 7.5 Hz, 4H), 2.2, (s, 3H), 2.25 (s, 3H), 4.78 (s, 2H), 5.2 (s, 2H), 6.48 (d, J = 8.5 Hz, 1H), 6.62 (d, J = 8.5 Hz, 1H), 6.8−6.9 (m, 4H), 7.18 (t, J = 8.3 Hz, 2H), 8.04 (m, 2H); ^{13}C NMR (400 MHz) δ 8.9, 17.1, 26.8, 43.7, 48.8, 70.0, 71.7, 110.5, 110.7, 116.2, 116.4, 126.3, 126.4, 126.5, 131.2, 131.3, 131.6, 141.8, 142.2, 154.2, 154.4, 194.4, 210.3; MS (ES) calculated for $C_{33}H_{39}FO_4Na$ 541.36, found 541.2 (M + Na).

3-[4-(2-Oxo-3,3-dimethylbutoxy)-3-methylphenyl)]-3-[4-(2-naphthylmethoxy)-3-methylphenyl]pentane (C-5). To a solution of 20 mg (0.057 mmol) of **2** in 0.26 mL of DMF was added 3 mg (0.078 mmol) of NaH. This mixture was stirred at room temperature for 30 min before 0.016 mL (0.068 mmol) of 2-(chloromethyl)naphthalene was added. The reaction was stirred for an additional 30 min before 2 mL of H_2O and 3 mL of EtOAc were added. The organic layer was washed with 1 mL of brine, dried over $MgSO_4$, and concentrated under reduced pressure. Purification by flash silica chromatography (10% EtOAc/hexanes) afforded 17 mg (51%) of **C-5** as a colorless oil. ^{1}H NMR (250 MHz) δ 0.65 (t, J = 7.0 Hz, 6H), 1.28 (s, 9H), 2.0 (q, J = 7.0 Hz, 4H), 2.22, (s, 3H), 2.25 (s, 3H), 4.8 (s, 2H), 5.48 (s, 2H), 6.5 (d, J = 8.5 Hz, 1H), 6.8−7.02 (m, 5H), 7.4−7.72 (m, 3H), 7.75−7.95 (m, 3H), 8.0−8.1 (m, 1H); ^{13}C NMR (400 MHz) δ 8.9, 17.1, 26.8, 29.7, 43.7, 48.8, 68.8, 70.0, 110.6, 124.0, 125.4, 125.7, 126.2, 126.3, 126.4, 126.6, 128.0, 128.4, 128.6, 131.0, 131.2, 131.9, 133.5, 134.1, 141.3, 142.0, 154.4, 155.0, 204.5; MS (ES) calculated for $C_{36}H_{42}O_3Na$ 545.4, found 545.2 (M + Na).

3-[4-(2-oxo-3,3-dimethylbutoxy)-3-methylphenyl)]-3-[4-(2-cyclohexylethoxy)-3-methylphenyl]pentane (C-6). To a solution of 20 mg (0.057 mmol) of **2** in 0.26 mL of DMF was added 3 mg (0.078 mmol) of NaH. The mixture was stirred at room temperature for 30 min before 9 μL (0.068 mmol) of 1-bromo-2-cyclohexylethane was added. The reaction was stirred for an additional 30 min before 2 mL of H_2O and 3 mL of EtOAc was added and the resulting organic layer was separated and washed with 1 mL of brine and dried over $MgSO_4$ and concentrated under reduced pressure. Purification by flash silica chromatography (10% EtOAc/hexanes) afforded 19 mg (67%) of **C-6** as a colorless oil. ^{1}H NMR (250 MHz) δ 0.58 (t, J = 7.5 Hz, 6H), 1.26 (s, 9H), 0.9−1.9 (m, 13H), 2.0 (q, J = 7.5 Hz, 4H), 2.2, (s, 3H), 2.25 (s, 3H), 3.98 (t, J = 7.5 Hz, 2H), 4.8 (s, 2H), 6.5 (d, J = 8.5 Hz, 1H), 6.68 (d, J = 8.5 Hz, 1H), 6.8−6.95 (m, 4H); ^{13}C NMR (250 MHz) δ 8.6, 16.7, 26.4, 26.6, 29.5, 33.4, 33.6, 34.9, 37.0, 43.4, 48.5, 64.3, 69.7, 109.8, 110.4, 125.4, 126, 130.4, 130.8, 140.3, 141.8, 154.0, 155.0, 210.1; MS (ES) calculated for $C_{33}H_{48}O_3Na$ 515.36, found 515.3 (M + Na).

3-[4-(2-Oxo-3,3-dimethylbutoxy)-3-methylphenyl)]-3-[4-(2-(2-naphthyl)-2-oxoethoxy)-3-methylphenyl]pentane (C-7). To a solution of 20 mg (0.057 mmol) of **2** in 0.26 mL of DMF was added 3 mg (0.078 mmol) of NaH. The mixture was stirred at room temperature for 30 min before 0.015 g (0.068 mmol) of 2-bromoacetonaphthone was added. The reaction was stirred for an additional 30 min before 2 mL of H_2O and 3 mL of EtOAc were added. The organic layer was washed with 1 mL of brine, dried over $MgSO_4$, and concentrated under reduced pressure. Purification by flash silica chromatography (10% EtOAc/hexanes) afforded 15 mg (50%) of **C-7** as a colorless oil. ^{1}H NMR (250 MHz) δ 0.50 (t, J = 7.5 Hz, 6H), 1.22 (s, 9H), 1.92 (q, J = 7.5 Hz, 4H), 2.22 (s, 6H), 4.75 (s, 2H), 5.25 (s, 2H), 6.48 (d, J = 8.5 Hz, 1H), 6.62 (d, J = 8.5 Hz, 1H), 6.75−7.0 (m 4H), 7.22−7.35 (m, 2H), 7.75−8.05 (m, 4H), 8.52 (s, 1H); ^{13}C NMR (400 MHz) δ 8.4, 16.7, 26.4, 29.2, 43.2, 48.4, 69.6, 71.5, 110.1, 110.4, 123.8, 125.3, 125.9, 126.0, 126.1, 126.9, 127.9, 128.2, 128.6, 128.8, 129.0, 130.7, 130.8, 132.1, 132.4, 135.8, 141.4, 141.7, 153.9, 154.0, 195.3, 210.1; MS (ES) calculated for $C_{37}H_{42}O_4Na$ 573.41, found 573.4 (M + Na).

3-[4-(2-Hydroxy-3,3-dimethylbutoxy)-3-methylphenyl)]-3-[4-(2-cyclohexylethoxy)-3-methylphenyl]pentane (C-8). To a 0 °C solution of 10 mg of **C-6** (0.019) in 0.1 mL of MeOH was added 1.5 mg (0.042 mmol) of $NaBH_4$. The mixture was stirred at 0 °C for 30 min before 1 mL of NH_4Cl and 3 mL of EtOAc were added. The organic layer

was washed with 1 mL of brine, dried over $MgSO_4$, and concentrated under reduced pressure. Purification by flash silica chromatography (20% EtOAc/hexanes) afforded 6 mg (64%) of **C-8** as a colorless oil. ^{1}H NMR (250 MHz) δ 0.58 (t, J = 7.5 Hz, 6H), 1.26 (s, 9H), 0.9−1.9 (m, 13H), 2.0 (q, = 7.5 Hz, 4H), 2.2, (s, 3H), 2.25 (s, 3H), 3.65−4.1 (m, 5H), 6.6−6.75 (m, 2H), 6.78−7.0 (m, 4H); ^{13}C NMR (250 MHz) δ 8.6, 16.7, 26.2, 29.5, 33.4, 33.6, 34.9, 37.0, 48.5, 65.9, 69.2, 109.8, 110.4, 125.6, 126.0, 126.2, 130.5, 130.7, 140.2, 141.4, 154.3, 155.0; MS (ES) calculated for $C_{33}H_{50}O_3Na$ 517.36, found 517.3 (M + Na).

3-[4-(2-Oxo-3,3-dimethylbutoxy)-3-methylphenyl)]-3-[4-(2-(2′,5′-dimethoxyphenyl)-2-oxoethoxy)-3-methylphenyl]pentane (C-9). To a solution of 20 mg (0.057 mmol) of **2** in 0.26 mL of DMF was added 3 mg (0.078 mmol) of NaH. The mixture was stirred at room temperature for 30 min before 18 mg (0.068 mmol) of 2′,5′-dimethoxy-2-bromoacetophenone was added. The reaction was stirred for an additional 30 min before 2 mL of H_2O and 3 mL of EtOAc were added. The organic layer was washed with 1 mL of brine, dried over $MgSO_4$, and concentrated under reduced pressure. Purification by flash silica chromatography (10% EtOAc/hexanes) afforded 15 mg (56%) of **C-9** as a colorless oil. ^{1}H NMR (250 MHz) δ 0.58 (t, J = 7.5 Hz, 6H), 1.28 (s, 9H), 2.1 (q, J = 7.5 Hz, 4H), 2.20 (s, 6H), 3.8 (s, 3H), 3.9, (s, 3H), 4.8 (s, 2H), 5.2 (s, 2H), 6.51 (m, 2H), 6.8−7.0 (m, 4H), 7.1 (d, J = 8.0 Hz, 1H), 7.32 (d, J = 8.0 Hz, 1H), 7.47 (s, 1H); ^{13}C NMR (400 MHz) δ 8.5, 16.6, 26.4, 29.3, 43.2, 48.4, 55.8, 56.0, 56.6, 69.6, 74.7, 110.1, 110.4, 112.9, 113.7, 121.6, 125.8, 125.9, 126.0, 126.1, 130.6, 130.8, 141.0, 141.6, 153.8, 153.9, 196.0, 212.1; MS (ES) calculated for $C_{35}H_{44}O_6Na$ 583.38, found 583.2 (M + Na).

Acknowledgment. pSG5hVDR was kindly provided by M. R. Haussler. We thank the National Institutes of Health (Grant No. RO1DK54257) for financial support.

Supporting Information Available: Copies of ^{1}H NMR and ^{13}C NMR spectra (PDF). This material is available free of charge via the Internet at http://pubs.acs.org.

JA0268377